

Three-Dimensional Human Tissue Models That Incorporate Diabetic Foot Ulcer-Derived Fibroblasts Mimic *In Vivo* Features of Chronic Wounds

Anna G. Maione, BA, PhD,¹ Yevgeny Brudno, PhD,^{2,3} Olivera Stojadinovic, MD,⁴
Lara K. Park, PhD,⁵ Avi Smith, BA,⁵ Ana Tellechea, PharmD, PhD,^{6,7} Ermelindo C. Leal, PhD,⁶
Cathal J. Kearney, PhD,^{2,3,8} Aristidis Veves, MD, DSc,⁶ Marjana Tomic-Canic, PhD,⁴
David J. Mooney, PhD,^{2,3} and Jonathan A. Garlick, PhD, DDS⁵

Diabetic foot ulcers (DFU) are a major, debilitating complication of diabetes mellitus. Unfortunately, many DFUs are refractory to existing treatments and frequently lead to amputation. The development of more effective therapies has been hampered by the lack of predictive *in vitro* methods to investigate the mechanisms underlying impaired healing. To address this need for realistic wound-healing models, we established patient-derived fibroblasts from DFUs and site-matched controls and used them to construct three-dimensional (3D) models of chronic wound healing. Incorporation of DFU-derived fibroblasts into these models accurately recapitulated the following key aspects of chronic ulcers: reduced stimulation of angiogenesis, increased keratinocyte proliferation, decreased re-epithelialization, and impaired extracellular matrix deposition. In addition to reflecting clinical attributes of DFUs, the wound-healing potential of DFU fibroblasts demonstrated in this suite of models correlated with *in vivo* wound closure in mice. Thus, the reported panel of 3D DFU models provides a more biologically relevant platform for elucidating the cell–cell and cell–matrix-related mechanisms responsible for chronic wound pathogenesis and may improve translation of *in vitro* findings into efficacious clinical applications.

Introduction

DIABETIC FOOT ULCERS (DFU) are a common and debilitating complication of diabetes.¹ Unfortunately, many DFUs remain refractory to current treatments, resulting in prolonged hospitalizations and amputation.¹ Many existing therapies are based on research conducted in two-dimensional (2D) monolayer cultures, which do not simulate the complexity of human skin and are not predictive of *in vivo* tissues responses.^{2,3} Three-dimensional (3D), tissue-engineered models more closely approximate the *in vivo* environment for studying skin and related tissues.² Use of 3D tissue models to investigate the behavior of cells derived

from chronic wounds could provide meaningful correlations between both *in vitro* and *in vivo* wound responses and better direct treatment strategies.

Fibroblasts are an important cell type in regulating the formation and healing of DFUs. Fibroblasts mediate numerous, essential repair processes that are altered in chronic wounds, such as cytokine secretion, stimulation of angiogenesis, support of re-epithelialization, and production and remodeling of extracellular matrix (ECM).⁴ Traditionally, the involvement of fibroblasts in these wound-healing processes has been studied in 2D monolayer cultures of fibroblast cell lines.⁵ However, the lack of dimensionality, cell–cell cross-talk, cell–matrix interactions, and disease-specific

¹Program in Cell, Molecular, and Developmental Biology, Sackler School of Graduate Biomedical Sciences, Tufts University, Boston, Massachusetts.

²Wyss Institute for Biologically Inspired Engineering, Harvard University, Boston, Massachusetts.

³School of Engineering and Applied Sciences, Harvard University, Cambridge, Massachusetts.

⁴Wound Healing and Regenerative Medicine Research Program, Department of Dermatology & Cutaneous Surgery, University of Miami Miller Medical School, Miami, Florida.

⁵Department of Oral and Maxillofacial Pathology, Oral Medicine and Craniofacial Pain, Tufts University School of Dental Medicine, Boston, Massachusetts.

⁶Microcirculation Laboratory and Joslin-Beth Israel Deaconess Foot Center, Beth Israel Deaconess Medical Center, Harvard Medical School, Boston, Massachusetts.

⁷Center for Neurosciences and Cell Biology, University of Coimbra, Coimbra, Portugal.

⁸Department of Anatomy, Royal College of Surgeons in Ireland, Dublin, Ireland.

cells provides a simplistic view of wound healing and limits the *in vivo* relevance of these findings. Thus, more realistic models that mimic the *in vivo* environment and cell behavior are needed to understand the multifaceted role of fibroblasts in wound pathogenesis.

Three-dimensional tissue models have been shown to accurately mimic features of *in vivo* cell physiology. Indeed, the morphology, gene expression, and signaling of fibroblasts grown in 3D environments are more similar to their *in vivo* counterparts than those grown in 2D monolayers.⁶ For example, human skin equivalent (HSE) tissues have been shown to mimic the heterotypic cross-talk between fibroblasts and keratinocytes that is required for epidermal stratification, differentiation, and epithelialization.² Tissue models have also been used to study fibroblast functions that rely on 3D tissue architecture, such as the deposition, assembly, and remodeling of ECM.^{7,8} However, 3D *in vitro* models have not been utilized to study fibroblast functions in chronic wound healing. Adaptation of such models to reflect features of the chronic wound environment will provide improved methods to investigate the impaired healing of DFUs.

To investigate the role of fibroblasts in DFUs, we isolated 12 primary fibroblast cell strains from DFU biopsies and from nonulcerated, site-matched skin of diabetic and non-diabetic patients. We demonstrated that these patient-derived fibroblasts exhibited differences in motility and cytokine secretion in 2D monolayer after expansion *in vitro*. While informative, these 2D models lacked the necessary complexity to investigate wound-healing processes such as angiogenesis, fibroblast-keratinocyte interactions, and ECM production. To more holistically investigate chronic wound repair, we incorporated the primary fibroblasts into 3D models and found they faithfully mimicked phenomena known to occur in chronic DFUs. Specifically, DFU-derived fibroblasts, in comparison to control fibroblasts, reduced stimulation of angiogenesis, increased proliferation of basal keratinocytes, impaired re-epithelialization, and decreased ECM production. The *in vivo* relevance of these findings was supported by the delayed healing of mouse wounds injected with DFU fibroblasts compared with those injected with nondiabetic control fibroblasts. Taken together, these results demonstrate proof of concept that the incorporation of primary DFU-derived fibroblasts into 3D tissue models recapitulates key aspects of the *in vivo* DFU microenvironment. Thus, these models may provide more biologically relevant experimental platforms for studying the mechanisms underlying DFU pathogenesis and could provide predictive paradigms for the discovery of more effective wound repair strategies.

Materials and Methods

Isolation of patient-derived fibroblasts and cell culture

Using a protocol approved by the Beth Israel Deaconess Medical Center Institutional Review Board, de-identified, discarded skin specimens were collected from routine surgical procedures, such as ulcer debridement, phalangectomy, bunionectomy, or arthroplasty. There are no safety concerns regarding participating subjects. Fibroblasts were isolated as previously described⁹ (see Supplementary Methods; Supplementary Data are available online at www.liebertpub.com/

tec). Fibroblasts were maintained in fibroblast growth media containing DMEM (1 g/L glucose) (Invitrogen, Carlsbad, CA), 10% fetal bovine serum (HyClone, Logan, UT), HEPES (Sigma-Aldrich, St. Louis, MO), and Pen/Strep/Fung (Invitrogen) at 37°C. All experiments were conducted on fibroblasts between passages 4 and 7.

Flow cytometry

See Supplementary Methods.

Scratch wound assay

See Supplementary Methods.

Antibody-based cytokine array and quantification

To characterize their secretory profiles, fibroblast strains (DFUF1, DFF6, and NFF10) were seeded at a density of 2×10^6 cells/100 mm on tissue culture plates in serum-free fibroblast growth media. Conditioned media was collected after 24 h and analyzed using the Proteome Profiler Human Cytokine Array Panel A kit (R&D Systems, Minneapolis, MN) according to the manufacturer's protocol. ImageJ software (NIH, Bethesda, MD) was used to quantify mean pixel intensity of duplicate cytokine spots and normalized to cell number.

Three-dimensional in vitro endothelial cell sprouting assay

To evaluate the ability of fibroblast strains to induce an angiogenic response, a 3D *in vitro* sprouting assay was modified from a previously described assay.¹⁰ Human umbilical vein endothelial cell-coated dextran beads were embedded in fibrin gel. In quadruplicate, fibroblasts (DFUF1, DFF6, or NFF10) were seeded on top of the gels at a density of 10,500 cells/cm² in a 1:1 mix of fibroblast growth media and EGM-2 media (final concentration: 1 g/L glucose, 6% serum). After 8 days, gels were fixed with 4% paraformaldehyde, stained with Hoechst dye, and visualized with an Olympus IX2 microscope. Endothelial sprouts were identified as continuous multi-cellular structures consisting of at least two cells that extended from the bead. Quantification is expressed as the mean \pm SD number of sprouts counted/number of beads counted (at least 60 beads were quantified per gel, and four gels were quantified per condition).

Three-dimensional HSEs fibroblast-keratinocyte cross-talk model

To evaluate fibroblast-keratinocyte cross-talk within a 3D skin-like environment, modified HSEs were constructed in triplicate wells as previously described.^{2,11} Briefly, fibroblasts (DFUF1, DFF6, or NFF10) were mixed with Type I Collagen (Organogenesis, Canton, MA) to a final concentration of 3×10^5 cells/mL. Submerged in epidermal growth media (containing 3.8 g/L glucose, 0.3% serum),^{2,11} the fibroblasts contracted and remodeled the collagen matrices over the course of 7 days. Then, 5×10^5 keratinocytes (normal human keratinocytes [NHKs]) isolated from human neonatal foreskin were seeded in 50 μ L of epidermal growth media on the surface of each collagen matrix. After 4 days, the constructs were raised to an air-liquid interface and fed

from the bottom with cornification media (containing 3.2 g/L glucose, 2% serum)^{2,11} to enable epithelial differentiation for 1 week. All tissues were pulsed with bromo-deoxyuridine (BrdU) (Invitrogen) for 6 h before fixation. Tissue sections stained by hematoxylin and eosin (H&E) were used to evaluate the stratification and differentiation of the epidermis. At least three sections of triplicate tissues were stained for BrdU incorporation using an anti-BrdU antibody (Roche, Indianapolis, IN). Images were taken with a Nikon Eclipse 80i microscope and Spot Advanced software (Diagnostic Instruments, Sterling Heights, MI). Quantification of BrdU was performed by counting the number of stained and unstained basal keratinocytes and expressed as mean percentage of basal keratinocytes positive for BrdU per 20× image ± SD.

Three-dimensional HSE tissue model of re-epithelialization

To measure fibroblast support of re-epithelialization, a 3D skin-like model of cutaneous wound healing was used as previously described.¹² Collagen “support” gels were seeded with fibroblasts (DFUF1, DFF6, or NFF10) at a final concentration of 3×10^5 cells/mL and were maintained submerged for 1 week in fibroblast growth media. HSE tissues constructed with human foreskin fibroblasts (HFFs), as described earlier,^{2,11} were wounded with a 5 mm biopsy punch and placed on the surface of the fibroblast-populated support gel. The wounded cultures were maintained at an air–liquid interface for 72 h and fed with fibroblast growth media (Supplementary Fig. S1). Tissues were then formalin fixed and paraffin embedded. Serial sections obtained from the midpoint of the wounds of triplicate tissues were stained by H&E, and percent wound closure was calculated by measuring the original wound size and the distance of epithelial tongue migration. Measurements are expressed as mean percent closure ± SD.

Construction of self-assembled ECM tissues

To assess the ability of fibroblasts to produce an ECM, we employed our model in which fibroblasts secrete and organize a 3D matrix, similar to that of granulation tissue.^{7,8} Fibroblasts (DFUF1, DFF6, or NFF10) were seeded in triplicate onto Millicell Hanging Cell Culture inserts (Milipore, Billerica, MA) (1.0-μM pore size) at a density of 5×10^5 cells/cm². Self-assembly media (1 g/L glucose, 5% serum) supplemented with 10 μg/mL ascorbic acid (Sigma-Aldrich) was changed every 3 days for 5 weeks⁸ (see Supplementary Methods for media formulation). Using ImageJ, at least three H&E stained sections per tissue were used to measure mean ECM thickness ± SD normalized to cell number.

Mouse wound-healing model

A mouse cutaneous wound-healing model was used to characterize the *in vivo* wound-healing potential of isolated fibroblasts. Sixteen-week-old C57BL6 male mice (Jackson Laboratories, Bar Harbor, ME) were anesthetized, and two 6-mm full-thickness skin punch biopsies were obtained from the shaved dorsum of the animals. DFUF1, DFF6, or NFF10 were combined with an alginate-based hydrogel formulation previously developed by our group¹³ (Supplementary

Methods). A total of 60 μL of blank hydrogel or cell-loaded hydrogel (1×10^6 cells/wound) was injected intradermally into three sites along the wound margins immediately after wound creation (day 0). The study groups were as follows: (1) blank hydrogel (vehicle only, $n=4$), (2) DFUF1-loaded hydrogel ($n=3$), (3) DFF6-loaded hydrogel ($n=4$), and (4) NFF10-loaded hydrogel ($n=5$). Healing was monitored over 10 days by daily wound tracing and is expressed as mean percentage of original wound size (day 0). Mice were euthanized at 10 days postwounding in order to collect wound tissue for histological analysis. All animal studies were conducted in accordance with Institutional Animal Care and Use Committee–approved protocols.

Statistics

Results are expressed as mean ± SD of at least three independent samples. All statistical analyses were conducted using IBM SPSS. One-way ANOVA and *post hoc* tests (Tukey’s HSD or Games–Howell) were used to determine statistical significance. For *in vivo* wound-healing data, mixed model analysis accounting for repeated measures over time was performed. * $p \leq 0.05$ and ** $p \leq 0.01$ were considered significant.

Results

Isolation of primary fibroblasts from three patient types for use in DFU models

We isolated three groups of primary dermal fibroblasts from patient biopsies: (1) Type II diabetic foot ulcer-derived fibroblasts (DFUF), (2) Type II diabetic, nonulcerated foot-derived fibroblasts (DFF), and (3) nondiabetic, nonulcerated foot-derived fibroblasts (NFF) for a total of 12 fibroblast strains (four in each group). Bright-field microscopy showed that isolated cells had a spindle-like morphology, typical of dermal fibroblasts (Supplementary Fig. S2). Due to the heterogeneous cell composition of the dermis, fibroblast purity was assessed by flow cytometry for mesenchymal markers expressed by skin fibroblasts (CD73, CD105, and CD140b) (Supplementary Table S1). A well-characterized HFF line served as a positive control for comparison. All patient-derived fibroblasts demonstrated high expression of mesenchymal markers with ≥99% positive for CD73, ≥95% positive for CD105, and ≥92% positive for CD140b, which was similar to that of control HFFs (95%, 95%, and 99% positive, respectively). To rule out the presence of contaminating cell types (ex. endothelial cells, macrophages, and lymphocytes), we examined expression of hematopoietic marker, CD31. All fibroblast cultures demonstrated low expression of the hematopoietic marker, with ≤3% of cells positive for CD31, similar to that of control HFFs (2% positive). There were no significant differences in expression of markers between fibroblast groups. These data indicate that cells isolated from patient biopsies were fibroblastic with minimal contaminating cell types.

DFUFs, DFFs, and NFFs retained phenotypic differences in 2D culture

To establish whether fibroblast strains retained phenotypic differences in 2D culture after *in vitro* expansion, we compared cell motility between DFUFs, DFFs, and NFFs

using a monolayer scratch wound assay. Supplementary Figure S3 shows representative bright-field images of scratches at 0 and 8 h postwounding. Quantification of percent closure revealed that 8 h postwounding, DFUFs and DFFs tended to repopulate the wound less than NFFs (Supplementary Fig. S3). Reduced cell motility could hinder wound repair, because fibroblasts would be less able to enter the wound bed and promote healing.⁴ These results support the fact that isolated fibroblasts preserve phenotypic differences in a 2D, monolayer culture consistent with their isolation source based on a previously reported work.^{5,14}

Based on the scratch wound assay data and a DNA methylation array (L.K.P. *et al.*, in review), we chose one representative strain from each fibroblast group, namely DFUF1, DFF6, and NFF10, for subsequent experiments and development of 3D models. To further demonstrate that phenotypic differences between fibroblast groups are maintained *in vitro*, a cytokine antibody array was used to assess their cytokine secretion profiles. Ten cytokines were detected in the fibroblast conditioned media (Fig. 1). Interleukin-8 (IL-8), monocyte chemotactic protein-1 (MCP-1), C-X-C motif chemokine 1 (CXCL1), and stromal-derived factor 1 (SDF-1) were secreted at higher levels by NFF10 compared with DFUF1 and DFF6, which had little to no detectable levels (Fig. 1). IL-6 secretion was not detectable in DFUF1 media, was found at an intermediate level in DFF6 media, and was at the highest level in NFF10 conditioned media. IL-23, plasminogen activator inhibitor-1 (PAI-1), macrophage migration inhibitory factor (MIF), interferon gamma (IFN- γ), and CD40 ligand were also detected; however, the differences in secretion between fibroblast strains were subtle. See Supplementary Figure S4 for a list of cytokines on the array that were not secreted by DFUF1, DFF6, or

NFF10 at a detectable level. These data show that DFUFs and DFFs have altered cytokine secretion *in vitro* which may have important implications for cell–cell cross-talk within 3D models and *in vivo* wound healing. Furthermore, these 2D assays demonstrate that fibroblast groups maintain phenotypic differences after expansion *in vitro* which could be reflective of their *in vivo* source. Although these 2D monolayer studies offer insights into chronic wound fibroblast physiology, they lack the complexity to fully evaluate wound-healing properties mediated through cell–cell and cell–matrix interactions. Thus, it is advantageous to use 3D models to more accurately study fibroblast functions in chronic wound repair.

DFUFs and DFFs induced less endothelial cell sprouting than NFFs in a 3D angiogenesis model

The cytokine array identified that DFUFs secreted less IL-6, IL-8, and SDF-1 than NFFs. Since these factors are involved in angiogenesis^{15–17} and their production is altered in DFUs,^{15,18} we hypothesized that altered cytokine secretion by DFUFs and DFFs would translate to decreased angiogenic induction in 3D models. To test this, we adapted an *in vitro* 3D angiogenesis assay.¹⁰ DFUF1, DFF6, or NFF10 were seeded on top of fibrin gels embedded with endothelial cell-coated beads and the number of endothelial cell sprouts was quantified as a measure of angiogenic induction. NFF10 stimulated endothelial cell sprouting to a greater extent than DFUF1 (3.7-fold greater) and DFF6 (1.6-fold greater) (Fig. 2). These results suggest that this model can be used to study cross-talk between endothelial cells and DFU-derived fibroblasts and how it may contribute to the impaired angiogenesis in chronic wounds.

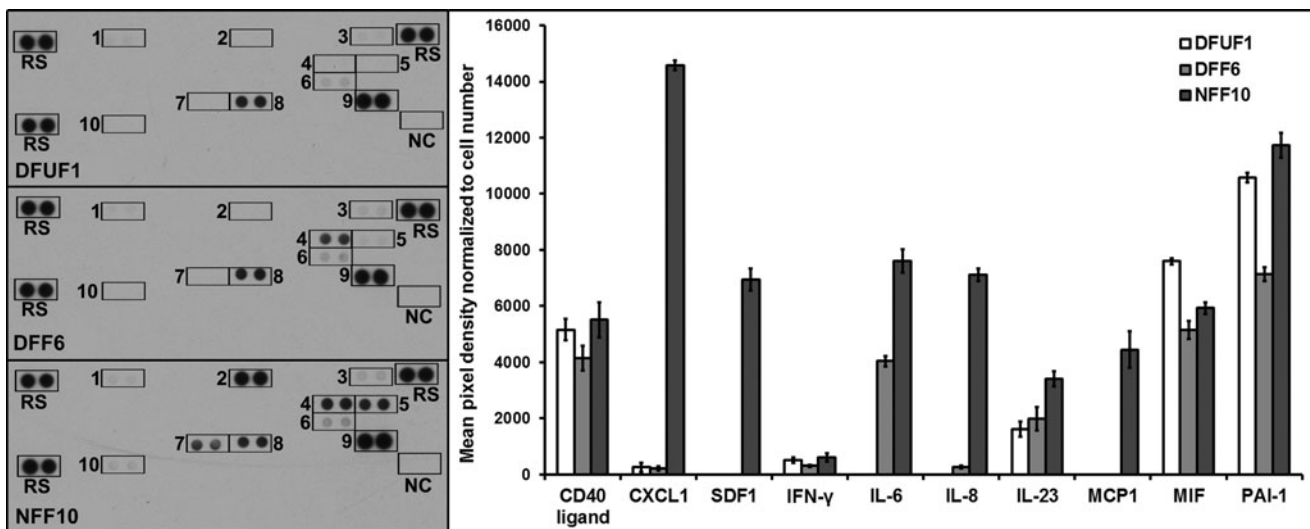


FIG. 1. DFUFs and DFFs displayed altered cytokine secretion *in vitro*. Images of cytokine array membranes used to analyze secretion profiles of DFUF1, DFF6, and NFF10 are shown. Antibody spot locations are labeled: 1 = CD40 Ligand, 2 = CXCL1, 3 = IFN- γ , 4 = IL-6, 5 = IL-8, 6 = IL-23, 7 = MCP-1, 8 = MIF, 9 = PAI-1, 10 = SDF-1, RS = Reference spots, and NC = Negative control. Densitometric quantification of array spots normalized to cell number revealed that DFUF1 and DFF6 exhibit altered secretory profiles compared with NFF10 in 2D monolayer culture *in vitro*. CXCL1, C-X-C motif chemokine 1; DFFs, type II diabetic, nonulcerated foot-derived fibroblasts; DFUFs, type II diabetic foot ulcer-derived fibroblasts; IFN- γ , interferon gamma; IL, interleukin; MCP-1, monocyte chemotactic protein-1; MIF, macrophage migration inhibitory factor; PAI-1, plasminogen activator inhibitor-1; SDF-1, stromal-derived factor 1.

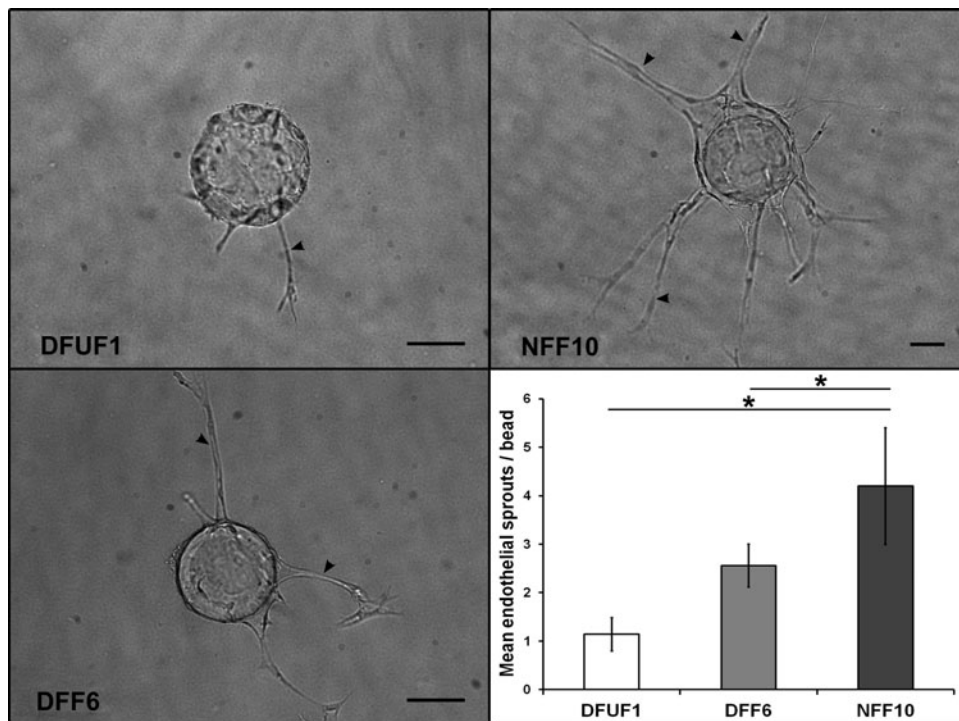


FIG. 2. DFUFs and DFFs promoted less endothelial cell sprouting than NFFs in a 3D angiogenesis model. Representative images of endothelial cell sprouts (arrowheads) off of dextran beads in fibrin gels in coculture with DFUF1, DFF6, or NFF10 are shown. Scale bars, 100 μ m. Quantification of mean number of endothelial sprouts per bead \pm SD ($n=4$) demonstrated that DFUF1 and DFF6 were less able to promote sprouting compared with NFF10. * $p < 0.05$. 3D, three dimensional; NFFs, nonulcerated foot-derived fibroblasts.

DFUFs induced proliferation of keratinocytes in HSK tissues

Given that fibroblasts communicate extensively with keratinocytes during healing and that keratinocytes at the periphery of chronic DFUs are often hyperproliferative,^{19–21} we tested whether DFUFs could induce this hallmark of chronic wounds in a 3D skin model. To mimic fibroblast-keratinocyte interactions that occur *in vivo*, we incorporated

DFUF1, DFF6, or NFF10 into collagen matrices of the dermal compartment of 3D HSE tissues. Healthy, human keratinocytes were seeded on the surface to form a stratified epithelium. Tissue sections demonstrated that all three fibroblast groups supported a well-organized, stratified epithelium. However, staining for BrdU incorporation revealed that basal keratinocytes in DFUF1-containing HSEs were 44% more proliferative than DFF6-HSEs and 47% more proliferative than NFF10-HSEs (Fig. 3). There was no

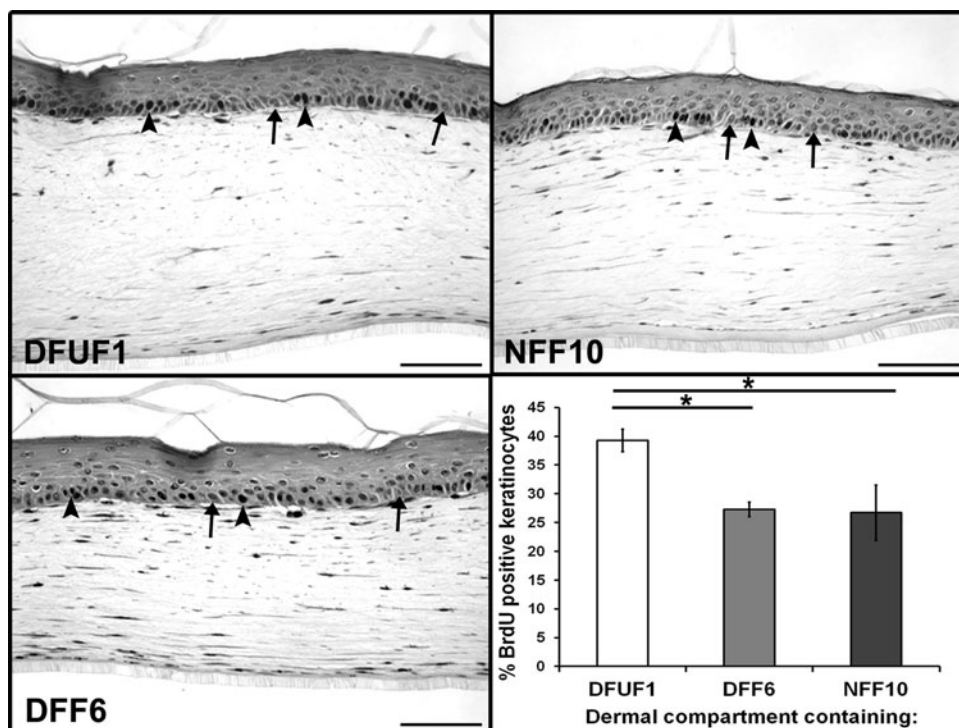


FIG. 3. DFUFs demonstrated increased basal keratinocyte proliferation in a 3D HSE model. HSE tissues were constructed with DFUF1, DFF6, or NFF10 in the dermal compartment. Representative images of tissue sections stained for BrdU incorporation are shown (arrowheads mark examples of BrdU-stained nuclei, and arrows mark examples of BrdU-negative nuclei). Scale bars, 100 μ m. Quantification of mean percentage of basal keratinocytes positive for BrdU \pm SD ($n=3$) revealed that keratinocytes in HSEs constructed with DFUF1 were more proliferative than those constructed with DFF6 or NFF10. * $p < 0.05$. BrdU, bromo-deoxyuridine; HSE, human skin equivalent.

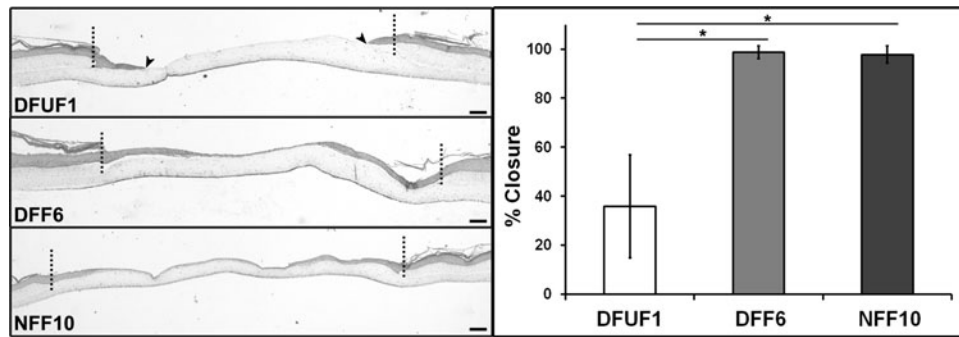


FIG. 4. DFUFs exhibited impaired support of re-epithelialization in a wounded HSE model. Representative H&E stained sections of 3D re-epithelialization tissue models constructed with DFUF1, DFF6, or NFF10 are shown. The *dotted line* demarcates the original wound edge. *Arrowheads* indicate migrating epithelial edge after 72 h on DFUF-supported wounds. Scale bars, 100 μ m. Quantification of re-epithelialization expressed as mean percent wound closure \pm SD ($n=3$) demonstrated that DFUF1 was less supportive of re-epithelialization compared with either DFF6 or NFF10. * $p < 0.05$. H&E, hematoxylin and eosin.

significant difference between DFF6- and NFF10-containing HSEs. These results suggest that DFUFs, but not DFFs, induce features of the chronic wound microenvironment in 3D HSE tissues, thereby providing a realistic model to study chronic wound fibroblast-keratinocyte interactions.

DFUFs displayed impaired support of re-epithelialization in a wounded HSE model

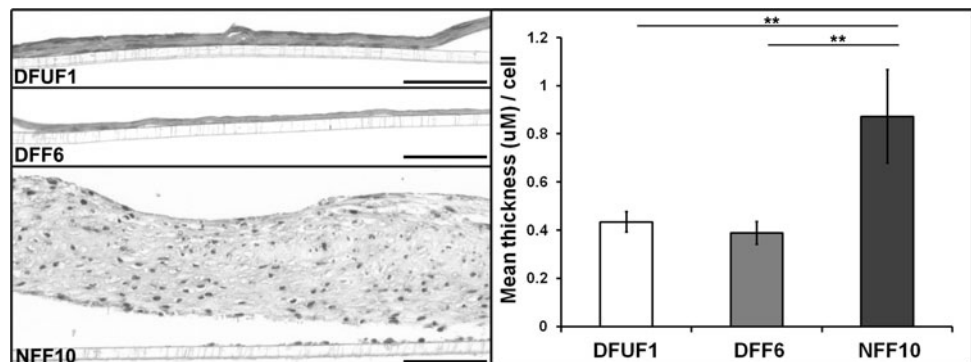
Since the epithelial phenotype was altered in the presence of DFUFs and re-epithelialization is known to be impaired in chronic wounds,¹⁹ we tested whether DFUFs would affect epithelial migration. To model re-epithelialization, we adapted our previously established 3D, *in vitro* model of excisional wound healing.¹² A biopsy punch was used to create a “full thickness” wound in the center of an HSE tissue. This “wounded” tissue was then placed on collagen “support” gels populated with DFUF1, DFF6, or NFF10 and average percent wound closure after 72 h was measured. Since HSEs constructed with DFUFs exhibited increased keratinocyte proliferation (Fig. 4), the wounded HSE tissues were constructed with healthy foreskin-derived fibroblasts and keratinocytes to provide a standardized wound tissue for comparing how DFUF, DFF, and NFF support re-epithelialization. H&E stained tissue sections showed that the epithelium completely or nearly completely closed the wounds on top of DFF6- and NFF10-populated gels (Fig. 4). However, the wounded epithelium on top of

DFUF1-populated gels only achieved an average of 36% wound closure (Fig. 4). This finding is consistent with the impaired re-epithelialization of DFUFs seen *in vivo* and demonstrates the utility of 3D HSE models for investigating how fibroblast-keratinocyte cross-talk mediates the chronic wound phenotype.

DFUFs and DFFs produced less ECM than NFFs in a 3D ECM assembly model

Since re-epithelialization *in vivo* is partially dependent on fibroblast production of ECM to act as a scaffold for keratinocyte migration,⁴ we assessed whether DFUFs exhibited abnormal ECM production. To address this in a biologically relevant setting, we utilized our previously established 3D *in vitro* assay of ECM production in which fibroblasts are stimulated with ascorbic acid for 5 weeks to secrete and assemble an ECM that is similar to wound granulation tissue.⁸ Examining sections of the fibroblast-produced ECM showed that DFUF1 and DFF6 produced thinner ECM compared with NFF10 (Fig. 5). Quantification of ECM thickness normalized to fibroblast number confirmed this observation (Fig. 5). These data are the first evidence that the impaired ECM phenotype associated with DFUFs²² may be due to decreased *de novo* ECM production by fibroblasts. This 3D ECM assembly model will be an invaluable tool for elucidating the nature of chronic wound ECM defects and their contribution to impaired healing.

FIG. 5. DFUFs and DFFs produced and assembled less ECM than NFFs. Representative H&E stained sections of ECM tissues created by DFUF1, DFF6, or NFF10 are shown. Scale bars, 100 μ m. Quantification of mean ECM area normalized to tissue length and cell number \pm SD ($n=3$). NFF10-produced ECMs were substantially thicker than those produced by either DFUF1 or DFF6. ** $p < 0.01$.



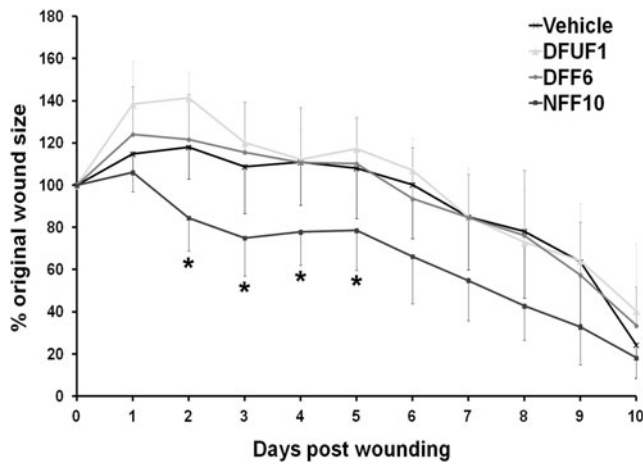


FIG. 6. Transplantation of NFFs correlated with improved wound closure *in vivo* compared with DFUFs and DFFs. Quantification of wound area (expressed as mean percentage of original wound size \pm SD) of full-thickness excisional wounds in mice after an injection of DFUF1 ($n=3$), DFF6 ($n=5$), NFF10 ($n=4$) in hydrogel, or hydrogel vehicle alone ($n=4$). NFF10 injection correlated with improved wound closure overall and specifically on days 2–5 postwounding compared with DFUF1, DFF6, or vehicle alone. $*p < 0.05$.

Transplantation of NFFs correlated with improved healing *in vivo* compared with DFUFs or DFFs

To determine whether the fibroblast phenotypes demonstrated in the 3D *in vitro* models translated to impaired healing *in vivo*, DFUF1, DFF6, and NFF10 were evaluated in a mouse model of cutaneous wound healing. Since the purpose of this experiment was to provide “proof-of-concept” and *in vivo* relevance for the 3D model results, not to demonstrate a therapeutic application, we chose to use a

full-thickness, excisional mouse wound model for its simplicity and ease of use. Before transplantation, we established that the fibroblasts were viable and motile within RGD-modified alginate hydrogel (Supplementary Fig. S5) over 10 days, suggesting it would be an appropriate vehicle for cell delivery. Hydrogel loaded with each fibroblast strain or hydrogel alone (control) was injected into the periphery of full-thickness excisional wounds on the dorsum of nondiabetic mice. A mixed model analysis of daily wound closure measurements revealed that an injection of NFF10 correlated with increased wound closure compared with an injection of DFUF1, DFF6, or hydrogel alone (Fig. 6). *Post hoc* tests for each time point determined that NFF10-injected wounds were significantly more healed than the other treatments on days 2–5 postwounding. By the 10th day, all treatment groups achieved similar amounts of wound closure, suggesting that the injected cells may affect early phases of wound healing, may be overwhelmed by local signaling, and/or are cleared by the immune system after several days *in vivo*. The differences in early wound healing demonstrated between DFUFs, DFFs, and NFFs are consistent with their performance in the 3D *in vitro* models, suggesting that these models may accurately reflect the *in vivo* healing potential of these cells.

Discussion

We developed 3D, biomimetic models that recapitulate key characteristics of the impaired healing of DFUs. Within these models, primary fibroblasts isolated from DFUs and site-matched diabetic and nondiabetic skin displayed phenotypic differences that are consistent with the impaired angiogenesis, hyperproliferation of keratinocytes, delayed re-epithelialization, and diminished ECM deposition associated with DFUs *in vivo* (see Table 1 for a summary of models presented). We validated that the impaired healing

TABLE 1. SUMMARY OF THREE-DIMENSIONAL *IN VITRO* MODELS AND RELATED REFERENCES

Model	Figure	Purpose	Analogous wound-healing process	Cell types used	References
Sprouting	Figure 2	To test the ability of fibroblasts to induce an angiogenic-like response in endothelial cells	Angiogenesis	HUVEC, DFUF/DFF/NFF	10,24,25
Human skin equivalent tissue	Figure 3	To examine the cross-talk between fibroblasts and keratinocytes in a skin-like tissue	Fibroblast-keratinocyte communication	NHKs, DFUF/DFF/NFF	2,11
Re-epithelialization	Figure 4, Supplementary Figure S1	To determine the ability of fibroblasts to support wound re-epithelialization	Re-epithelialization	NHKs, HFFs, DFUF/DFF/NFF	12,28,29
Self-assembled ECM	Figure 5	To evaluate fibroblast capacity to synthesize and assemble ECM <i>de novo</i>	Granulation tissue production	DFUF/DFF/NFF	7,8

DFFs, type ii diabetic, nonulcerated foot-derived fibroblasts; DFUFs, type II diabetic foot ulcer-derived fibroblasts; ECM, extracellular matrix; HFF, human foreskin fibroblast; HUVEC, human umbilical vein endothelial cell; nondiabetic, NFF, nonulcerated foot-derived fibroblasts; NHKs, normal human keratinocytes.

phenotypes exhibited in our models correlates with *in vivo* wound-healing potential using a mouse cutaneous wound-healing model. Since these 3D models accurately mimic aspects of DFU wound healing, they can be used to interrogate the fibroblast functions and molecular mechanisms responsible for these healing defects. Thus, these models will play a key role in the identification of potential therapeutic targets that can be further investigated and verified using suitable animal wound-healing models.

Previous studies have implied that fibroblasts in a diabetic environment may contribute to the impaired angiogenesis and vasculogenesis of chronic wounds.²³ Specifically, diabetic mouse fibroblasts grown in a 2D monolayer secrete less vascular endothelial growth factor, a prominent pro-angiogenic factor.¹⁴ Similar to our cytokine array results, fibroblasts in diabetic mouse wounds produce less SDF-1, which is important in recruiting endothelial progenitor cells to the wound bed.¹⁷ We and others have previously shown that human fibroblasts promote an angiogenic-like response in endothelial cells using a 3D endothelial cell sprouting assay.^{24,25} By adapting this model, we provide evidence that DFU-derived fibroblasts directly decrease the angiogenic response of endothelial cells. This suggests that altered fibroblast-endothelial cell signaling may be involved in impaired revascularization of DFUs *in vivo*. The benefit of this 3D assay is that it accurately recapitulates several steps of *in vivo* angiogenesis,²⁴ thereby providing a more realistic setting to study fibroblast and endothelial cell interactions as they occur in chronic wounds.

In addition to fibroblast-endothelial cell interactions, fibroblasts communicate with keratinocytes to facilitate healthy wound healing.²¹ Soluble factors known to signal between fibroblasts and keratinocytes during acute wound healing are differentially expressed in chronic wounds.^{18,15} Likewise, we have shown altered cytokine secretion by primary DFU-derived fibroblasts using a cytokine array. Furthermore, the epidermis at the margins of chronic wounds is frequently abnormal; exhibiting hyperproliferation, hyperkeratosis, parakeratosis, and aberrant gene expression.^{19,26,27} Unfortunately, conventional, 2D, monolayer cultures have not been able to mimic these epidermal features. To better model chronic wound fibroblast-keratinocyte interactions, we employed 3D HSE tissues that have been shown to mimic the form and function of human skin, including fibroblast support of epidermal differentiation and stratification.² Incorporation of DFU-derived fibroblasts into 3D HSEs resulted in increased basal keratinocyte proliferation, similar to the hyperproliferative epidermis of calluses found surrounding chronic ulcers.²⁰ Our finding suggests that DFU-derived fibroblasts may be sufficient to promote this DFU epidermal phenotype. Based on these results, 3D HSE tissues provide a realistic representation of fibroblast-keratinocyte interactions in the DFU microenvironment and may facilitate mechanistic studies into the role of these interactions in chronic wound repair.

Despite hyperproliferation of keratinocytes, re-epithelialization of DFUs is delayed or even completely impaired, as has been observed clinically and in *ex vivo* models.^{19,26} Proper re-epithelialization of acute wounds is partially mediated by fibroblast-keratinocyte signaling.²¹ To determine whether altered fibroblast-keratinocyte signaling impairs DFU re-epithelialization, we employed a 3D wounded HSE

model previously shown to mimic cutaneous excisional wound healing.^{12,28} Until now, monolayer scratch wound assays have been used to characterize the retarded planar cell motility of chronic wound-derived keratinocytes.^{19,20} However, our model provides a more biologically relevant context to study epithelial migration as a sheet and enables us to examine the support of this process by DFU-derived fibroblasts.²⁹ We found that incorporation of DFU-derived fibroblasts into this model recapitulated the impaired wound closure of DFUs. As we have previously shown that fibroblast-keratinocyte cross-talk directs re-epithelialization in this model,^{12,28} our results further substantiate that DFU-derived fibroblasts have altered communication with keratinocytes. Incorporating DFU-derived fibroblasts into wounded 3D HSE tissues mimics the impaired re-epithelialization of a chronic wound and, thus, can serve as an important tool for elucidating the mechanisms that impair chronic wound closure.

It is important to note that both fibroblast-keratinocyte cross-talk and re-epithelialization models are constructed with keratinocytes isolated from healthy donors, as it is technically challenging to isolate and expand keratinocytes from DFU biopsies. However, the fact that healthy keratinocytes exhibited DFU-related phenotypes in 3D coculture with DFU-derived fibroblasts highlights the significant effect of DFU-derived fibroblast on keratinocytes. Another important aspect of the re-epithelialization model is that healthy foreskin fibroblasts were used to construct the wounded HSEs. By eliminating any confounding effects due to differences in HSE construction, such as the increased basal keratinocyte proliferation seen in DFUF-populated HSEs, we could specifically examine the supportive role of DFUFs, DFFs, and NFFs in re-epithelialization. In addition, the use of HSEs constructed with healthy NHKs and HFFs provided a standardized baseline for comparing wound re-epithelialization between the three fibroblast groups. A future direction of this work is to create a re-epithelialization model using DFUFs, DFFs, or NFFs in both the wounded HSE and the support gel to better reflect the *in vivo* diabetic wound environment.

In addition to cell-cell signaling, fibroblasts support wound closure through their secretion, deposition, and remodeling of ECM, which provides a scaffold and stimulation for cell migration and proliferation.⁴ While morphologic analysis of patient biopsies have provided some evidence that the ECM composition is altered and that levels of matrix degrading enzymes are elevated in chronic DFUs,^{15,22,30} the *de novo* production of ECM by DFU-derived fibroblasts has not been examined. Using a 3D model of ECM deposition and assembly that we previously have shown to produce an ECM similar to wound granulation tissue,⁸ we demonstrated that DFU- and diabetic-derived fibroblasts exhibit a deficiency in *de novo* ECM synthesis. This suggests that the aberrant ECM phenotype of chronic wounds may be partly attributed to diminished ECM deposition by fibroblasts in the diabetic environment. The advantage of using this ECM model over conventional assays that measure secretion of soluble ECM proteins in monolayer culture is that it assesses the capacity of fibroblasts to assemble ECM proteins into a functional, *in vivo*-like, 3D matrix. In future studies, this model can be used to more fully characterize the ECM defects of DFU-derived

fibroblasts and the signaling pathways that may be modulated to improve them.

This work establishes that primary fibroblast strains isolated from DFUs and site-matched controls are a valuable resource for studying the nature and potential mechanisms of impaired DFU healing when integrated into 3D tissue models. In our 3D tissue models, these fibroblasts exhibit properties that are consistent with the *in vivo* DFU phenotype after expansion *in vitro*. The retention of such attributes *in vitro* may occur through a phenomenon called metabolic memory, in which cells exposed to hyperglycemic conditions, similar to those found in diabetic patients, undergo changes, such as epigenetic modifications, which are sustained long after they are removed from that environment.^{31,32} Although metabolic memory has primarily been demonstrated in vascular cells,³³ there is some evidence that fibroblasts retain functional changes, such as altered ECM production, after exposure to high glucose.^{34,35} Therefore, metabolic memory may play a role in maintaining the phenotype of DFU-derived fibroblasts in our *in vitro* tissue models. Further studies using these models are necessary to determine whether and how metabolic memory mediates the long-term effects of the DFU microenvironment manifested in the 3D models.

Since primary fibroblasts may retain biological properties of their *in vivo* environment, the three fibroblast groups, DFUF, DFF, and NFF, offer important insights into the differential effects of the diabetic and ulcer microenvironments. For instance, DFUFs and DFFs performed similarly to each other and different from NFFs in the angiogenesis model, ECM model, and mouse wound-healing model. This may imply that the diabetic microenvironment from which DFUFs and DFFs were isolated specifically affects these wound-healing processes. However, in the 3D HSE tissues and re-epithelialization model, the DFFs performed more similarly to the NFFs than to the DFUFs. This may suggest that the ulcer microenvironment, more than the diabetic microenvironment, affects functions mediated by fibroblast-keratinocyte cross-talk. By comparing DFUFs and DFFs, we can begin to tease apart the particular effects of the chronic ulcer and diabetic environments on fibroblast wound-healing functions. These differences also emphasize the need for a suite of 3D models, as not all wound-healing processes are affected similarly.

In summary, we demonstrated that 3D, *in vitro* models incorporating primary DFU-derived fibroblasts provide biologically relevant insights into the role of fibroblasts in mediating DFU pathologies. The benefit of these 3D models is that they better mimic the *in vivo* tissue microenvironment and reciprocal cell–cell interactions compared with monolayer cultures. In addition, these biomimetic models use human cells, are standardized, and are easy to manipulate and interpret, which may help reduce the need for large-scale animal studies. In combination, these models offer a comprehensive approach to understand DFU pathogenesis, aid in the identification of predictive biomarkers, and facilitate the discovery of more effective treatment strategies. These 3D models also can be easily adapted to study physiological and pathological processes of skin and other stratified epithelial tissues, thereby extending their utility to a diverse range of biological applications. Ultimately, these biomimetic models are a valuable platform for wound-

healing research and the translation of more efficacious therapeutics.

Acknowledgments

The authors would like to acknowledge J. Barretto, E.B. Knight, V. Yanez, A. Miller, I. Jozic, L. Liang, J. DeFuria, and J. Edwards for their contributions and assistance. This work was supported by grant no. DK098055-06A1 to J.A.G. from the National Institute of Health (NIH).

Authors' Contributions

A.G.M. conceived and designed the experiments, collected and assembled data, analyzed and interpreted data, wrote the manuscript, and gave final manuscript approval. Y.B. conceived, collected, and interpreted data. O.S. collected and assembled data and reviewed the manuscript. L.K.P. interpreted and performed statistical analysis of data. A.S. collected data. A.T. collected and assembled data. E.C.L. collected and assembled data. C.J.K. collected, assembled, and interpreted data. A.V., M.T.C., and D.J.M. conceived and designed the study, interpreted data, obtained financial support, and provided manuscript feedback. J.A.G. conceived and designed the study, interpreted data, obtained financial support, wrote the manuscript, and gave final manuscript approval. J.A.G. is the guarantor of this work and, as such, had full access to all the data in the study and takes responsibility for the integrity of the data and the accuracy of the data analysis.

Disclosure Statement

No competing financial interests exist.

References

1. Boulton, A.J.M., Vileikyte, L., Ragnarson-Tennvall, G., and Apelqvist, J. The global burden of diabetic foot disease. *Lancet* **366**, 1719, 2005.
2. Carlson, M.W., Alt-Holland, A., Egles, C., and Garlick, J.A. Three-dimensional tissue models of normal and diseased skin. *Curr Protoc Cell Biol Editor Board Juan Bonifacino* **Chapter 19**, Unit 19.9 2008.
3. Breslin, S., and O'Driscoll, L. Three-dimensional cell culture: the missing link in drug discovery. *Drug Discov Today* **18**, 240, 2013.
4. Singer, A.J., and Clark, R.A. Cutaneous wound healing. *N Engl J Med* **341**, 738, 1999.
5. Brem, H., *et al.* Primary cultured fibroblasts derived from patients with chronic wounds: a methodology to produce human cell lines and test putative growth factor therapy such as GM-CSF. *J Transl Med* **6**, 75, 2008.
6. Green, J.A., and Yamada, K.M. Three-dimensional microenvironments modulate fibroblast signaling responses. *Adv Drug Deliv Rev* **59**, 1293, 2007.
7. Pouyani, T., *et al.* *De novo* synthesis of human dermis *in vitro* in the absence of a three-dimensional scaffold. *In Vitro Cell Dev Biol Anim* **45**, 430, 2009.
8. Shamis, Y., *et al.* iPSC-derived fibroblasts demonstrate augmented production and assembly of extracellular matrix proteins. *In Vitro Cell Dev Biol Anim* **48**, 112, 2012.
9. Proia, D.A., and Kuperwasser, C. Reconstruction of human mammary tissues in a mouse model. *Nat Protoc* **1**, 206, 2006.

10. Brudno, Y., Ennett-Shepard, A.B., Chen, R.R., Aizenberg, M., and Mooney, D.J. Enhancing microvascular formation and vessel maturation through temporal control over multiple pro-angiogenic and pro-maturation factors. *Biomaterials* **34**, 9201, 2013.
11. Segal, N., *et al.* The basement membrane microenvironment directs the normalization and survival of bioengineered human skin equivalents. *Matrix Biol J Int Soc Matrix Biol* **27**, 163, 2008.
12. Egles, C., Garlick, J.A., and Shamis, Y. Three-dimensional human tissue models of wounded skin. *Methods Mol Biol Clifton NJ* **585**, 345, 2010.
13. Kong, H.J., Kaigler, D., Kim, K., and Mooney, D.J. Controlling rigidity and degradation of alginate hydrogels via molecular weight distribution. *Biomacromolecules* **5**, 1720, 2004.
14. Lerman, O.Z., Galiano, R.D., Armour, M., Levine, J.P., and Gurtner, G.C. Cellular dysfunction in the diabetic fibroblast: impairment in migration, vascular endothelial growth factor production, and response to hypoxia. *Am J Pathol* **162**, 303, 2003.
15. Blakytyn, R., and Jude, E. The molecular biology of chronic wounds and delayed healing in diabetes. *Diabet Med J Br Diabet Assoc* **23**, 594, 2006.
16. Koch, A., *et al.* Interleukin-8 as a macrophage-derived mediator of angiogenesis. *Science* **258**, 1798, 1992.
17. Gallagher, K.A., *et al.* Diabetic impairments in NO-mediated endothelial progenitor cell mobilization and homing are reversed by hyperoxia and SDF-1 alpha. *J Clin Invest* **117**, 1249, 2007.
18. Dinh, T., *et al.* Mechanisms involved in the development and healing of diabetic foot ulceration. *Diabetes* **61**, 2937, 2012.
19. Stojadinovic, O., *et al.* Molecular pathogenesis of chronic wounds: the role of beta-catenin and c-myc in the inhibition of epithelialization and wound healing. *Am J Pathol* **167**, 59, 2005.
20. Usui, M.L., Mansbridge, J.N., Carter, W.G., Fujita, M., and Olerud, J.E. Keratinocyte migration, proliferation, and differentiation in chronic ulcers from patients with diabetes and normal wounds. *J Histochem Cytochem Off J Histochem Soc* **56**, 687, 2008.
21. Werner, S., Krieg, T., and Smola, H. Keratinocyte-fibroblast interactions in wound healing. *J Invest Dermatol* **127**, 998, 2007.
22. Loots, M.A., *et al.* Differences in cellular infiltrate and extracellular matrix of chronic diabetic and venous ulcers versus acute wounds. *J Invest Dermatol* **111**, 850, 1998.
23. Kota, S.K., *et al.* Aberrant angiogenesis: the gateway to diabetic complications. *Indian J Endocrinol Metab* **16**, 918, 2012.
24. Nakatsu, M.N., *et al.* Angiogenic sprouting and capillary lumen formation modeled by human umbilical vein endothelial cells (HUVEC) in fibrin gels: the role of fibroblasts and Angiopoietin-1. *Microvasc Res* **66**, 102, 2003.
25. Shamis, Y., *et al.* Fibroblasts derived from human pluripotent stem cells activate angiogenic responses *in vitro* and *in vivo*. *PLoS One* **8**, e83755, 2013.
26. Stojadinovic, O., Zabelinski, M., and Tomic-Canic, M. Healing competence of the keratinocytes and the chronic wound edge. *Adv Wound Care* **1**, 171, 2010.
27. Stojadinovic, O., *et al.* Dereglulation of keratinocyte differentiation and activation: a hallmark of venous ulcers. *J Cell Mol Med* **12**, 2675, 2008.
28. Garlick, J.A. Engineering skin to study human disease—tissue models for cancer biology and wound repair. *Adv Biochem Eng Biotechnol* **103**, 207, 2007.
29. Safferling, K., *et al.* Wound healing revised: a novel re-epithelialization mechanism revealed by *in vitro* and *in silico* models. *J Cell Biol* **203**, 691, 2013.
30. Lobmann, R., *et al.* Expression of matrix-metalloproteinases and their inhibitors in the wounds of diabetic and non-diabetic patients. *Diabetologia* **45**, 1011, 2002.
31. Engerman, R.L., and Kern, T.S. Progression of incipient diabetic retinopathy during good glycemic control. *Diabetes* **36**, 808, 1987.
32. Pirola, L., Balcerzyk, A., Okabe, J., and El-Osta, A. Epigenetic phenomena linked to diabetic complications. *Nat Rev Endocrinol* **6**, 665, 2010.
33. Pirola, L., *et al.* Genome-wide analysis distinguishes hyperglycemia regulated epigenetic signatures of primary vascular cells. *Genome Res* **21**, 1601, 2011.
34. Benazzoug, Y., Borchiellini, C., Labat-Robert, J., Robert, L., and Kern, P. Effect of high-glucose concentrations on the expression of collagens and fibronectin by fibroblasts in culture. *Exp Gerontol* **33**, 445, 1998.
35. Yevdokimova, N.Y. High glucose-induced alterations of extracellular matrix of human skin fibroblasts are not dependent on TSP-1-TGFbeta1 pathway. *J Diabetes Complications* **17**, 355, 2003.
36. Bouhadir, K., *et al.* Degradation of partially oxidized alginate and its potential application for tissue engineering. *Biotechnol Prog* **17**, 945, 2001.
37. Rowley, J.A., Madlambayan, G., and Mooney, D.J. Alginate hydrogels as synthetic extracellular matrix materials. *Biomaterials* **20**, 45, 1999.

Address correspondence to:

Jonathan A. Garlick, PhD, DDS

Department of Oral and Maxillofacial Pathology

Oral Medicine and Craniofacial Pain

School of Dental Medicine

Tufts University

55 Kneeland St., South Cove, Room 116

Boston, MA, 02111

E-mail: jonathan.garlick@tufts.edu

Received: July 12, 2014

Accepted: October 14, 2014

Online Publication Date: March 30, 2015